Journal of Fluorescence, Vol. 8, No. 3, 1998

Dynamics of Trp Residues in Crystals of Human α_1-Acid Glycoprotein (Orosomucoid) Followed by Red-Edge Excitation Spectra

J. R. Albani[1]

Received January 6, 1998; revised May 28, 1998; accepted June 9, 1998

The present work reports for the first time the development of a method that allowed us to obtain crystals of orosomucoid complexed to progesterone. Then we investigated the dynamics of the microenvironments of the two buried Trp residues in the crystals of protein, by the red-edge excitation spectra method. The fluorescence excitation spectrum of the crystals is characteristic of that known for Trp residues (λ_{max} = 290 nm and bandwidth = 38 ± 1 nm), indicating that the Trp residues are responsible for the fluorescence of the protein in the crystals. The position of the maximum and the bandwidth of the steady-state emission spectrum of the crystals (331 ± 1 and 43 ± 1 nm, respectively) are equal to those obtained in aqueous buffer for the orosomucoid–progesterone complex (330 ± 1 and 43 ± 1 nm) (λ_{ex}, 295 nm). Thus, the fluorescence of the crystals occurs from the Trp residues buried in the protein core. The red-edge excitation spectra studies indicate that the Trp residues are surrounded by microenvironments that display motions, a result identical to that observed in solution. Thus, the crystallization process does not modify the structure or the dynamics of orosomucoid core. The fluorescence intensities depend on the angular orientation of the crystals with respect to the polarization of the incident beam. The general feature of this dependence is identical at the three excitation wavelengths used (295, 300, and 305 nm). Our results confirm the fact that the local structure and dynamics are the key for any interpretation of tryptophan fluorescence parameters of orosomucoid.

KEY WORDS: Tryptophan fluorescence; orosomucoid-progesterone crystals; protein dynamics; red-edge excitation spectra.

INTRODUCTION

The human α_1-acid glycoprotein (orosomucoid), a plasma glycoprotein of molecular weight equal to 41 kDa, consists of a chain of 181 amino- acids. It contains 40% carbohydrate, by weight, and has up to 16 sialic acid residues (10–14%, by weight) [1]. Five heteropolysaccharide groups are linked via N-glycosidic bond to the asparaginyl residues of the protein [2]. This high degree of sialylation and the presence of acidic amino-acid residues give rise to a very low p*I* of 2.8–3.8 [3;4].

Although the biological function of orosomucoid is still obscure, a number of activities of possible physiological significance have been described such as the ability to bind immunoglobulins G 3 [5], the β-drug adrenergic blocker, propranolol [6], and steroïd hormones such as progesterone [7].

α_1-Acid glycoprotein contains three Trp residues, one at the surface and two embedded in the protein matrix [1,2,8]. The dynamic behavior of each class of tryptophanyl residues was investigated by performing steady-state measurements of emission anisotropy be-

[1] Laboratoire de Biophysique Moléculaire, Université des Sciences et Technologies de Lille, B.P. 649, 59656 Villeneuve d'Ascq Cédex, France, Fax: 33320459218.

1053-0509/98/0900-0213$15.00/0

tween −40 and 20°C. This method allows to derive parameters characteristic of the environment of the rotating unit, such as the thermal coefficient of the frictional resistance to the rotation of the fluorophore and the characteristic amplitude at which the surrounding amino acids become the determinant of that frictional resistance [9]. Our results have shown that both classes of Trp residues exhibit residual motions, although the Trp residue of the surface rotates much more freely than the buried ones [10].

Binding of progesterone to orosomucoid partially quenches the Trp residues fluorescence [1]. Recently, we measured the steady-state fluorescence anisotropy of the Trp residues of orosomucoid in the presence of progesterone between −40 and + 6°C. Our results indicate that binding of the ligand to the protein decreases the frictional resistance of the buried Trp residues and increases that of the surface Trp residue. These results demonstrate that binding of progesterone to orosomucoid affects the dynamics of both the surface and the protein core [11].

We also characterized the emission spectrum of each class of fluorophore in the absence and in the presence of the ligand. We found that binding of progesterone to orosomucoid induces a red shift of 6 nm of the emission of the buried Trp residues (from 324 to 330 nm) and a blue shift of 5 nm of the emission of the surface Trp residue (from 350 to 345 nm). Thus, binding of progesterone affects the local structures around the Trp residues. However, the fluorescence maximum of the spectrum of the protein does not change whether or not the progesterone is bound to orosomucoid (λ_{max} = 333 ± 1 nm) [11].

In addition to the anisotropy experiments, dynamics of proteins can be investigated also by the red-edge excitation spectra method [12].

Excitation at the red edge of the absorption spectrum of the fluorophore molecules allows study of the flexibility of their microenvironment. When a fluorophore exhibits free motions, the position of the maximum of its fluorescence spectrum does not vary with the excitation wavelength. However, in a viscous or rigid medium, the fluorescence maximum position shifts to higher wavelengths upon red-edge excitation [13–21].

In the red-edge excitation spectral studies, the subject being studied is the relaxation of the environment (which consists of amino acids and solvent dipoles) around the excited tryptophan. In the fluorescence anisotropy experiments, on the other hand, the displacement of the emission dipole moment of the tryptophan is monitored. In the first approach it is the dynamics of the environment that is being followed, and in the second approach, the restricted reorientational motion of the Trp.

The crystallization of orosomucoid proved to be somewhat difficult, probably because of the high solubility and the large carbohydrate moiety of the protein. By using lead ion (0.007 *M*), the solubility of orosomucoid is reduced significantly, approximately equal to the effect of 40% ethanol. Also, the addition of a mixture of equal amounts of acetone and methanol decreases the solubility much further, to yield crystals under appropriate conditions [22].

However, because of the difficulty in obtaining the crystals, since 1953, crystallization of orosomucoid has not been performed. Therefore, there are no structural or dynamical studies (such as X-ray diffraction, NMR, or fluorescence) on crystals of orosomucoid.

The present work reports the development of a method that allowed us to obtain crystals of orosomucoid complexed to progesterone. Furthermore, we investigated here the dynamics of the microenvironments of the two buried Trp residues in the crystals of the protein–progesterone complex, by the red-edge excitation spectra method [23].

The fluorescence excitation spectrum of the crystals is characteristic of that known for Trp residues (λ_{max} = 290 nm and bandwidth = 38 ± 1 nm), indicating that the Trp residues are responsible for the fluorescence of the protein in the crystals.

The position of the maximum and the bandwidth of the steady-state emission spectrum of the crystals (331 ± 1 and 43 ± 1 nm, respectively) are equal to those obtained in aqueous buffer for the two buried Trp residues in orosomucoid–progesterone complex (330 ± 1 and 43 ± 1 nm, respectively). Thus, in the crystals, the Trp residue at the protein surface does not fluoresce.

The dynamics studies were performed on the crystals after we rotated them around the excitation beam of vertical polarization. Our results indicate that the buried Trp residues are surrounded by microenvironments that display mean motions, a result identical to that observed in solution.

Our results indicate that crystallization process does not modify the structure and the dynamics of orosomucoid core.

MATERIALS AND METHODS

Orosomucoid was extracted from human plasma and prepared as described in Ref. 7.

Progesterone (from Sigma) was dissolved in methanol. The concentration of the stock solution was 2.5 m*M*.

Crystallization of orosomucoid was performed following the procedure of Schmidt [22], with some modifications. Our crystals were obtained as follows: 32 mg of the lyophilized protein was dissolved in 460 μl of twice-distilled water, 30 μl of the stock solution of progesterone was then added to the solution of orosomucoid, and finally, 12 μl of a 1 *M* lead acetate solution was mixed with the orosomucoid–progesterone complex. The final solution was kept at 5°C for 2 h. Three hundred microliters of a precooled (5°C) mixture of methanol–acetone (1:1) was then added drop by drop, with careful stirring. The final solution was kept at 5°C for 1 year. During this time important crystals of orosomucoid–progesterone complex were formed (Fig. 1)

Fluorescence spectra were obtained with a Perkin–Elmer LS-5B spectrofluorometer. Bandwidths used for excitation and emission were 5 nm.

Crystals were mounted on a micropipette cone and were placed in the center of the cuvette holder of the fluorometer. Observed fluorescence intensities were corrected for the background intensities of a crystallized buffer solution, obtained at saturated concentrations of sodium phosphate buffer.

All experiments were performed at 22 ± 1°C.

RESULTS

Protein Preparation

Crystals of orosomucoid–progesterone obtained after 1 year of growth are displayed in Fig. 1. The organization of the protein in the crystals was identified by small- and wide-angle x-ray diffraction studies (J. R. Albani and R. Martinez, paper in preparation). Briefly, the results show that both protein moiety and glycan residues are crystallized. The proteins are linked together by the glycans, a phenomenon already observed in other glycoproteins [24–28]. The volume of one protein within the crystal was determined to be equal to 81,680 Å^3, a value close to that (72,453 Å^3) of a spherical protein of molecular weight equal to 41,000. Thus, the crystal volume per unit molecular weight, V_m, was calculated to be 1.99 Å^3/Da, which corresponds to a solvent of about 35%. This value is within the normal range for protein crystals [29–32].

Progesterone, a hydrophobic ligand, was added to the solution of orosomucoid in order to decrease the hydrophilicity of the protein and to facilitate its crystallization. Since we did not attempt to prepare the crystals without adding progesterone, we are not able, for the moment, to define the role of the ligand in the procedure of crystallization.

Fluorescence Excitation and Emission Spectra

Figure 2 displays the fluorescence excitation spectrum of the crystallized orosomucoid. The value of the bandwidth (38 ± 1 nm) indicates that the Trp residues are responsible for the fluorescence of the protein in the crystal.

The steady-state emission spectrum of the crystals obtained by exciting with unpolarized light (Fig. 3a) is identical to that obtained in aqueous buffer for the two buried Trp residues (Fig. 3b), having an emission maximum at 331 ± 1 and 330 ± 1 nm, respectively (λ_{ex}, 295 nm) and a bandwidth equal to 43 ± 1 nm. In solution, the emission maximum of orosomucoid–progesterone complex is equal to 332 ± 1 nm and the bandwidth is 56 nm [11] (see also Fig. 3d). Thus, the fluorescence observed for the crystal is characteristic of Trp residues embedded in the protein matrix [33].

When excitation was performed with a vertical polarized light, whether on solution of orosomucoid or on the crystal, the bandwidths of the spectra are 10 nm smaller than those observed when the spectra were recorded with unpolarized light. In the crystal, the bandwidth is equal to 35 ± 1 nm (Fig. 4a) instead of 43 ± 1 nm (Fig. 3a), and in solution, it is equal to 41 ± 1 nm (Fig. 4b) instead of 54 ± 1 nm (Fig. 3c). We do not know whether this phenomenon is due to the polarizer used or not. Figure 4c exhibits the fluorescence spectra of solution of orosomucoid obtained with unpolarized light (A) and with vertically polarized light (B). Although the bandwidth decreases when excitation light is polarized, in solution and in the crystals, the fluorescence emission maximum does not change with the nature of the excitation light. In the dynamics studies, excitation was performed with a vertically polarized light.

Excitation at 300 nm gives an emission maximum in the same range as that obtained with excitation at 295 nm. Therefore, there is no evidence of tyrosine fluorescence contribution at excitation wavelengths equal to or higher than 295 nm. This contribution may account for a blue-shifted spectrum.

Dynamics of the Microenvironments of the Buried Trp Residues

The red-edge excitation spectra method is used to monitor motions around the fluorophores [10–21]. Trp residues and their direct microenvironment (which con-

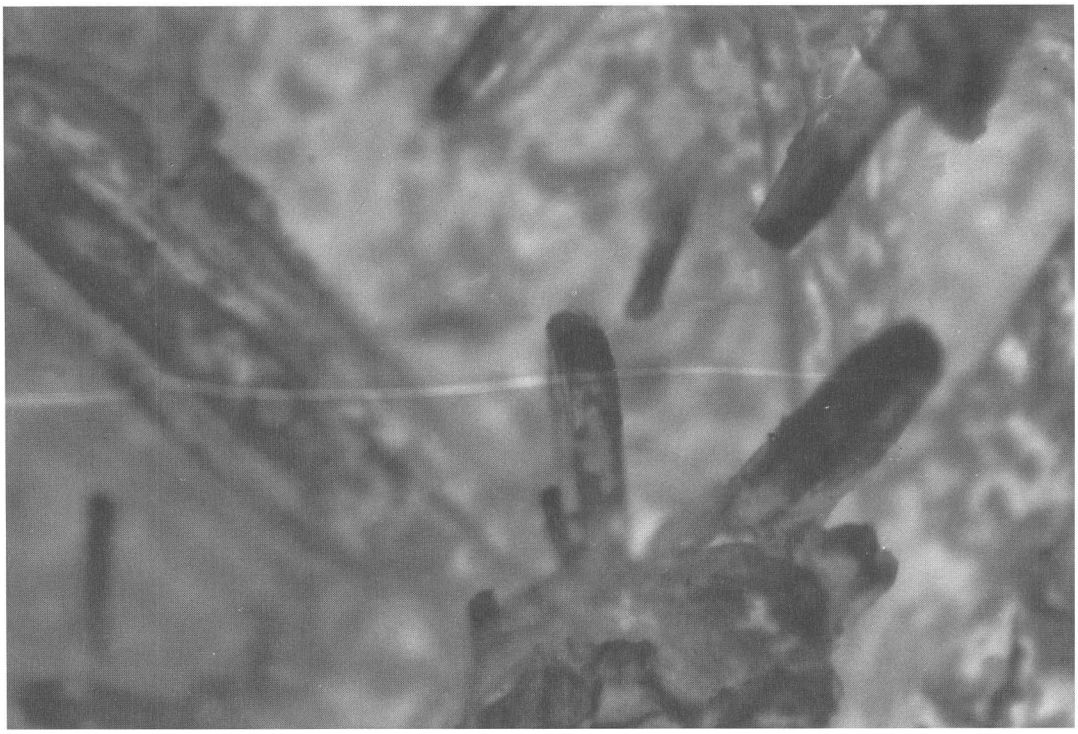

Fig. 1. Photograph (×57) of crystals of orosomucoid–progesterone complex, obtained in the presence of lead acetate.

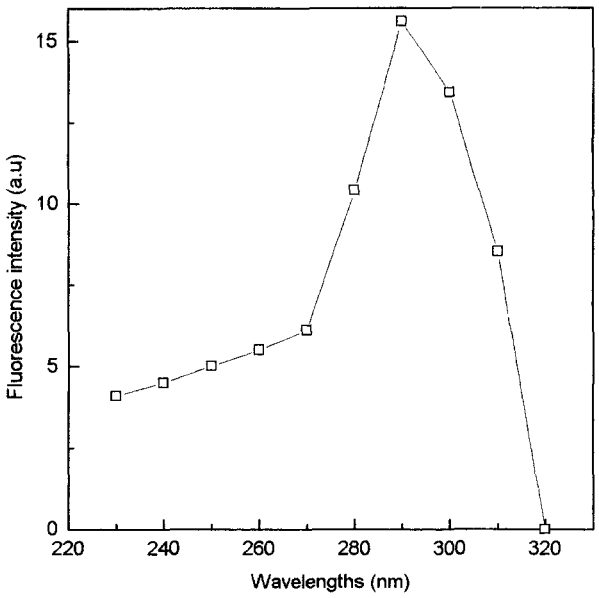

Fig. 2. Fluorescence excitation spectrum of a crystal of orosomucoid–progesterone complex. λ_{em} = 335 nm. Excitation and emission slits were 5 nm. The spectrum was recorded by excitation with unpolarized light.

sists of the dipole of both surrounding amino acids and solvent molecules in case of the exposed Trp residues) are associated by their dipoles. The dipoles referred here are the result of the charge distribution in the molecular plane. The excitation of the solution results in a redistribution of electronic charge on the fluorophore, inducing a significant change in both direction and strength of its dipole moment. If the dipole of the fluorophore microenvironment is able to relax before fluorophore emission, then this environment is considered to be fluid. This motion may induce that of the tryptophan. The emission maximum from a relaxed state does not change with the excitation wavelength, while an emission maximum from a nonrelaxed state will depend on it. Emission maxima are compared only if the spectra are symmetric. Otherwise, the centers of gravity should be compared.

Figure 5 displays the fluorescence spectra of Trp residues of crystals of orosomucoid–progesterone complex obtained by exciting with vertically polarized light at three excitation wavelengths, 295, 300, and 305 nm. The maximum (331 nm) of the tryptophan fluorescence of the crystals does not change with the excitation wavelength. The same result was obtained in the absence and presence of progesterone for orosomucoid in solution

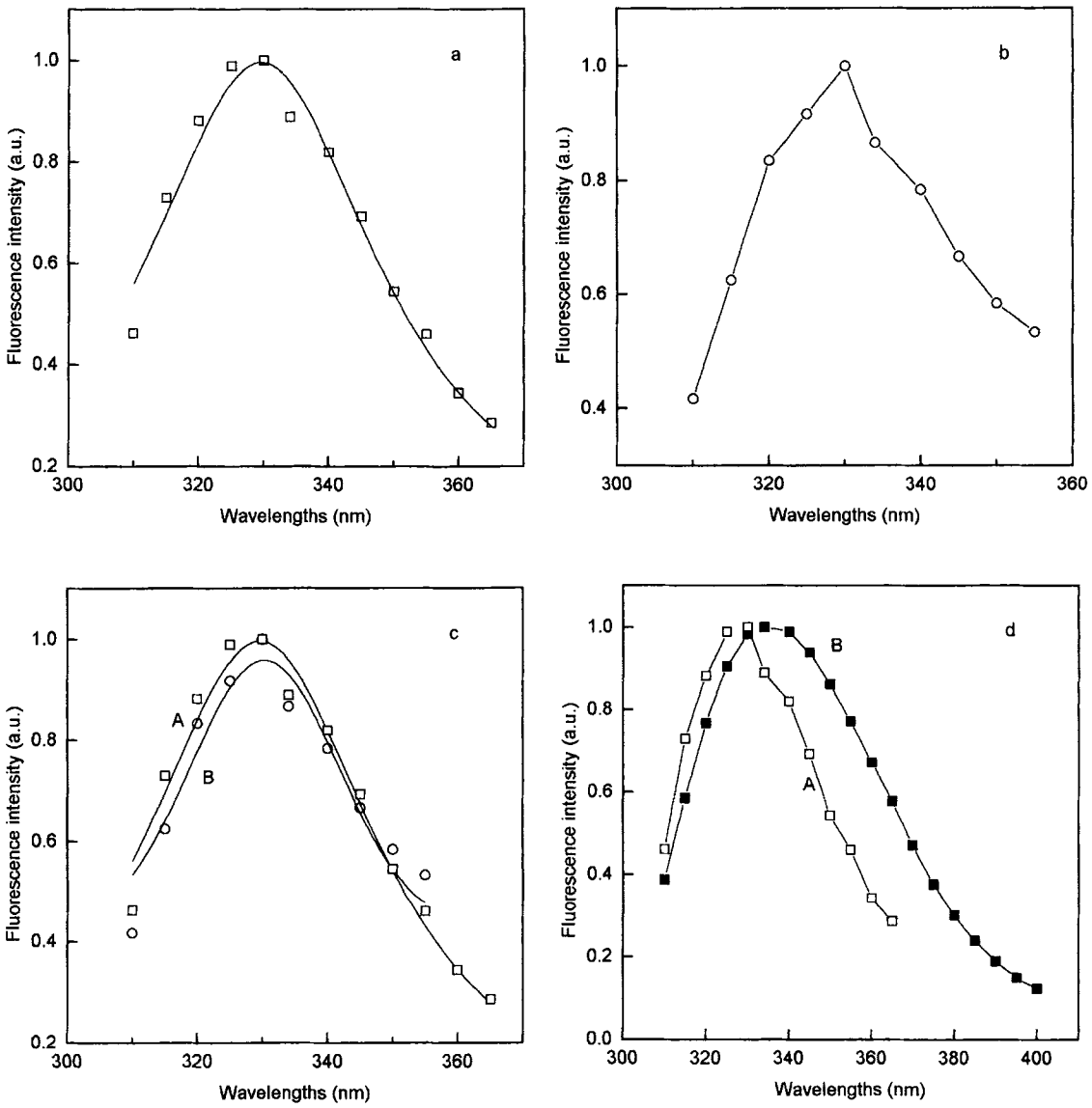

Fig. 3. Fluorescence emission spectra of a crystal of orosomucoid–progesterone complex (λ_{em}, 331 nm; and bandwidth = 43 nm) (a) and of the two buried Trp residues in a solution of orosomucoid–progesterone complex (λ_{em}, 330 nm; bandwidth = 43 nm) (b). λ_{ex} = 295 nm. Excitation and emission slits were 5 nm. The spectrum of the crystal was recorded by exciting the sample with unpolarized light. Spectrum b was obtained from fluorescence intensity quenching by cesium of a solution of orosomucoid–progesterone complex, after extrapolating to $[Cs^+] = \infty$ as indicated in Ref. 11. The spectra obtained from the crystal and from the solution are displayed together in (c) (A and B, respectively). (d) exhibits the fluorescence emission spectra of crystals of orosomucoid–progesterone complex (A) and of a solution of orosomucoid–progesterone complex (B), both obtained at an excitation wavelength of 295 nm with unpolarized light.

[10,11,21,34]. As the emission spectra are asymmetric, we converted them to a wavenumber scale,

$$\nu = 1/\lambda \qquad (1)$$

then we compared the positions of their centers of gravity or mean wavenumber $\bar{\nu}$.

$$\bar{\nu} = \Sigma I_i \nu_i / \Sigma I_i \qquad (2)$$

where I_i is the fluorescence intensity at the wavenumber ν_i. The values of the centers of gravity are 3.0208×10^4 cm^{-1} (331 nm), 3.015×10^4 cm^{-1} (331.7 nm), and 3.0303×10^4 cm^{-1} (330 nm) at λ_{ex} 295, 300, and 305 nm, respectively.

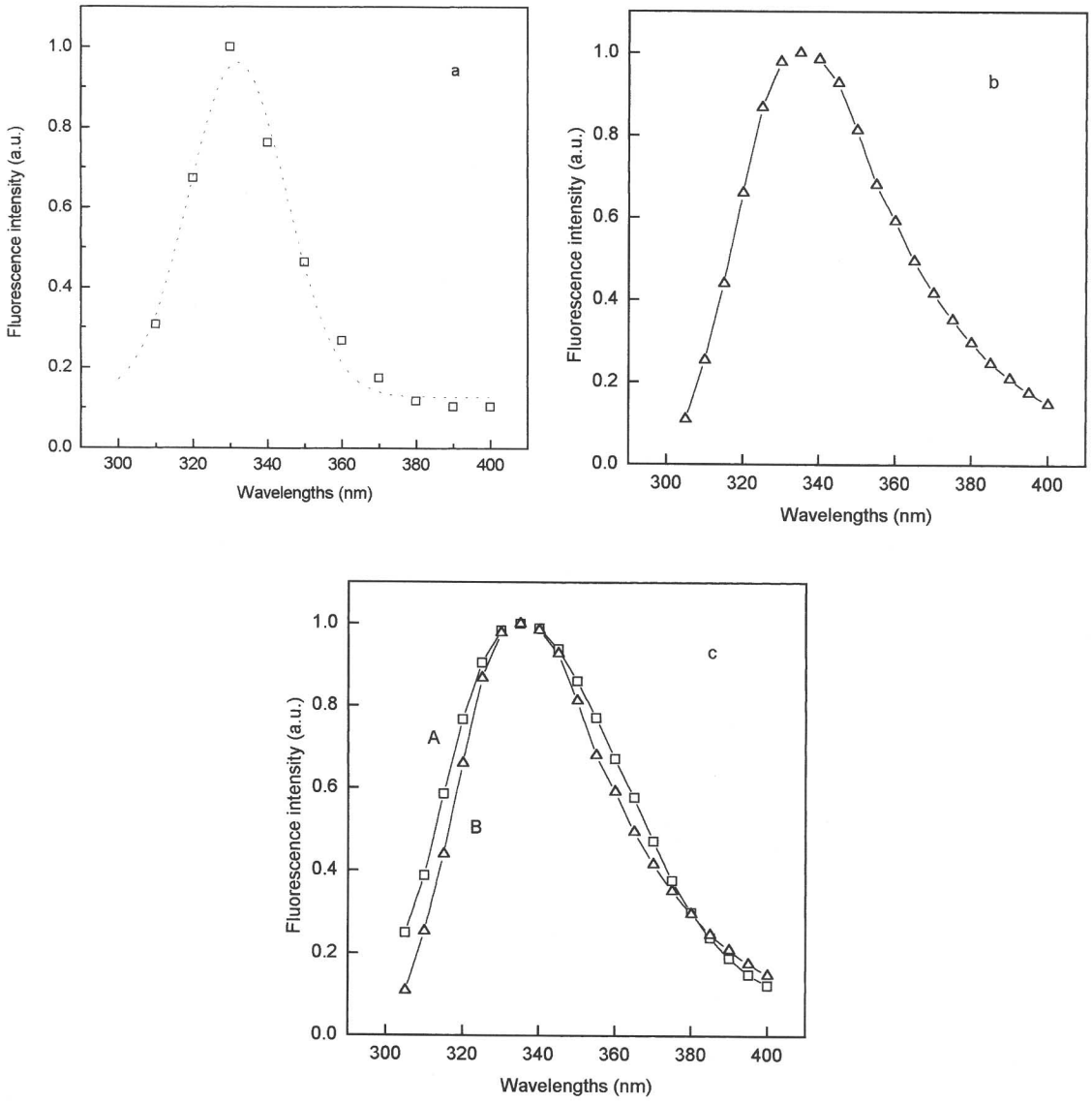

Fig. 4. Steady-state fluorescence emission spectra of crystals of orosomucoid–progesterone complex (λ_{max}, 330 nm; bandwidth = 35 ± 1 nm) (a) and of a solution of orosomucoid–progesterone complex (λ_{max}, 332 ± 1 nm; bandwidth = 41 nm) (b), both recorded with a vertically polarized excitation light. The excitation wavelength used for the two spectra is 295 nm. (c) displays the spectra of orosomucoid–progesterone in solution obtained with unpolarized light (A) and with vertically polarized excitation light (B).

Figure 5 exhibits the calculated emission spectra (dashed lines) obtained by assuming the position of the maximum equal to the center of gravity. Since the center of gravity of the fluorescence spectrum does not change with the excitation wavelength, emission occurs after relaxation process. In this case, the emission energy and thus the emission maximum and the center of gravity of the spectrum are independent of the excitation wavelength. Therefore, our results indicate that the microenvironment of the Trp residues is not rigid. This is in good agreement with those found in solution for orosomucoid prepared by chromatographic methods. Since we are observing the emission from the two buried Trp residues, we are monitoring the dynamics around both Trp residues. The red-edge excitation spectra method gives information on the mean motion of the microen-

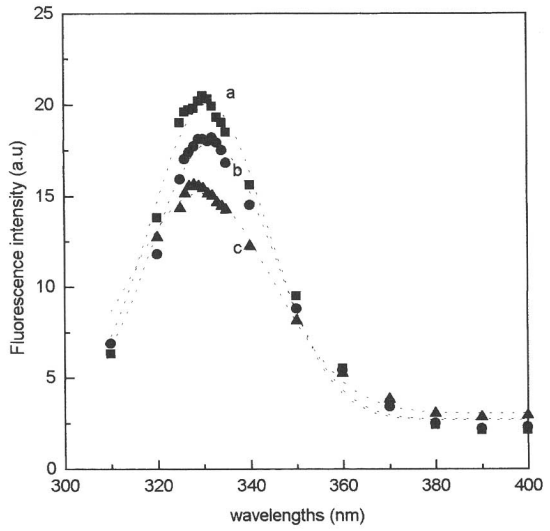

Fig. 5. Steady-state fluorescence emission spectra of a crystal of orosomucoid, recorded at three excitation wavelengths, 295 nm (a), 300 nm (b), and 305 nm (c). The dotted lines show the spectra obtained by considering the maximum equal to the centers of gravity, 331, 331.7, and 330 nm, at λ_{ex} 295, 300, and 305 nm, respectively. Excitation and emission slits were 5 nm. The spectra were obtained with a vertically excitation light.

vironment of the Trp residues, the method does not allow to study the dynamic behaviour of each tryptophanyl residue.

Rotation of the crystal around the excitation beam by steps of 45 ± 5° does not induce any modification in the red-edge excitation spectra results. At all angles (0, 45, 90, 135, and 180°), no shift was observed either in the fluorescence maximum or in the center of gravity of the spectrum (Figs. 6A–E). This result indicates clearly that at all the angles we are monitoring the dynamics of the same microenvironments of the Trp residues in the crystal of protein. At all angles, we are exciting the dipoles of the two buried Trp residues.

Tryptophan has two overlapping $S_o \rightarrow S_1$ electronic transitions (^1L_a and ^1L_b) which are perpendicular to each other [35–38]. Both the $S_o \rightarrow {}^1L_a$ and the $S_o \rightarrow {}^1L_b$ transitions occur in the 260- to 300-nm range. In polar solvents, ^1L_a has a lower energy than ^1L_b, and emission from this lowest state will be observed. Since the fluorescence intensity of a fluorophore is proportional to the square of the absorption transition probability, then it should vary with the angular dependence of the fluorophore's dipole with respect to the direction of the excitation beam. If the orientation of the dipoles of the Trp residues is modified as the result of the motion of the Trp residues, then the fluorescence intensity will change with the angle of the rotation of the crystal. In the absence of motions, the fluorescence intensity will remain constant at all positions of the crystal, since we are monitoring a definite orientation of the dipoles. One also should note that we are monitoring the fluorescence of two Trp residues. Therefore, the fluorescence intensity variation, if any, will be the result of the relative mobility of each Trp residues.

The fluorescence intensity variation as a function of angles of rotation obtained at three excitation wavelengths, 295, 300, and 305 nm, is shown in Fig. 7. The dynamics of the microenvironment of the Trp residues will induce the motion of the fluorophore. This motion, within the nanosecond range, will modify the orientation of its corresponding dipole, thus affecting its absorption and its emission. Since we have two Trp residues, the results obtained in Fig. 7 clearly indicate that at least one dipole is changing its orientation with time as the result of the dynamics of the corresponding Trp residue.

DISCUSSION

In 1953, F. Schmid [22] described a method of crystallization where the solution is heated in order to dissolve the orosomucoid and to evaporate the methanol–acetone mixture. We attempted to crystallize the protein by following the same procedure without any success. We reached 70°C and failed to obtain a limpid solution. We repeated the experiment five times without any success.

In our procedure, we did not heat the solution, but we performed a slow evaporation at 5°C. The important growth of the crystals could be the result of the slow growth at low temperatures. The presence of a high concentration of carbohydrate in orosomucoid plays an important role in the global crystallization and induces the spacial conformation and orientation of the protein in the crystal [39].

In principle, in order to observe an "entity" with x-ray diffraction studies, its mobility within the crystal should be reduced. For example, flavocytochrome b_2, the *L*(+)-lactate: cytochrome *c* oxidoreductase (EC. 1.1.2.3), is a tetrameric enzyme (M_r, 235 kDa) containing one flavin monomucleotide (FMN) and one protoheme IX per protomer [40]. The enzyme can be cleaved by controlled proteolysis into two functional derivatives: the cytochrome b_2 core, a monomer of molecular mass equal to 14 kDa; and flavodehydrogenase, a tetramer of molecular mass equal to 160 kDa [41]. Each protomer of the flavodehydrogenase binds one cytochrome b_2

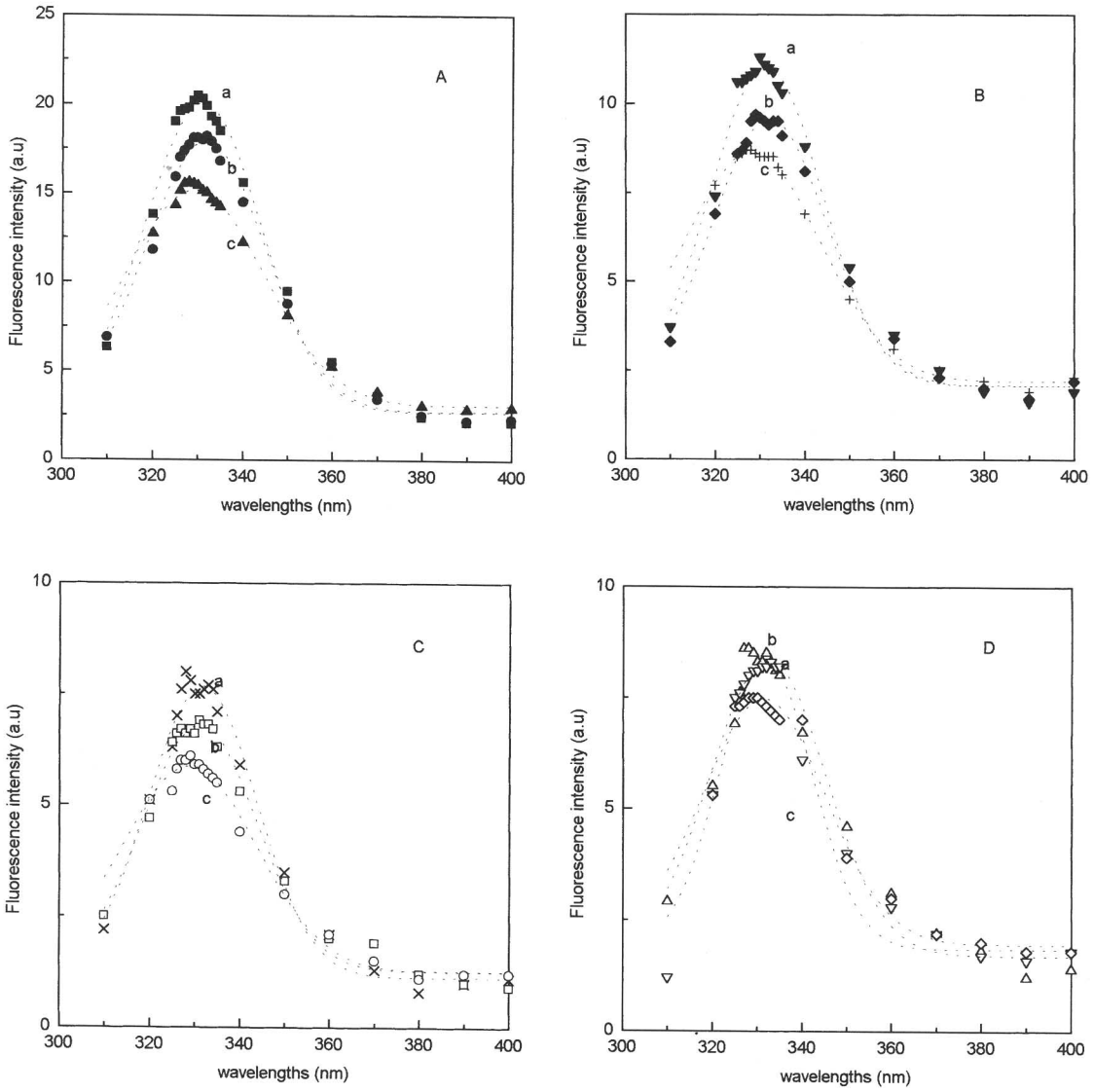

Fig. 6. Steady-state fluorescence spectra of a crystal of orosomucoid, recorded at three excitation wavelengths, 295 (a), 300 (b), and 305 nm (c), and at different angular position of the crystal relative to the excitation beam of vertically polarized light. (A) 0°, (B) 45°, (C) 90°, (D) 135°, and (E) 180°. The error in the value of the angles was estimated to be ± 5°. The plots in A are the same as those shown in Fig. 5.

core. The x-ray diffraction studies performed on flavocytochrome b_2 from *Saccharomyces cerevisae* indicated that two cytochrome b_2 cores are well ordered in the crystal lattice and the two others are disordered, completely absent from the electron density map [42].

Fluorescence titration of flavodehydrogenase–2-*p*-toluidinylnaphthalene-6-sulfonate (TNS) complex with cytochrome b_2 core showed that there are two classes of cytochromes with different affinities for the flavodehydrogenase protomers. The two cytochromes of higher affinity bind tightly to the flavodehydrogenase subunits, giving a well—ordered entity in the crystal lattice. The two other cytochromes, with a low affinity, display constant motions inducing the formation of a complex of shorter lifetime with the flavodehydrogenase protomers [43]. This complex would not be observed in x-ray diffraction studies [42].

In glycoproteins, the heterogeneity and the motions of glycans are two major problems for structural studies. Heterogeneous glycans represent an obstacle for crys-

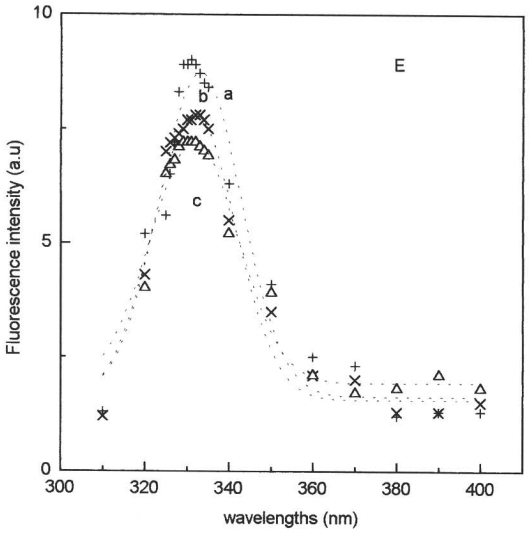

Fig. 6. Continued.

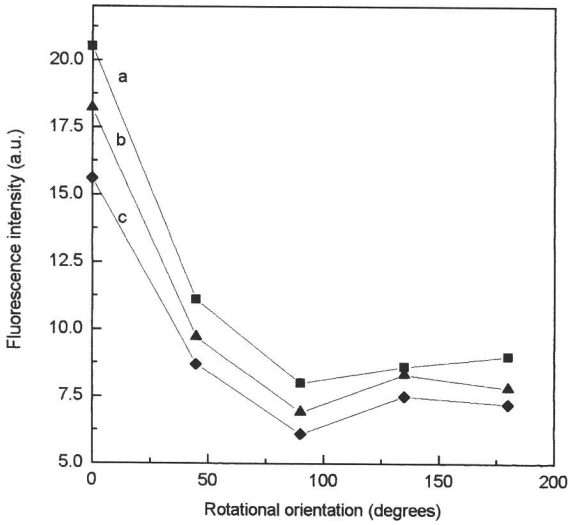

Fig. 7. Dependence of the fluorescence intensity on the crystal orientation with respect to the vertical direction of the excitation light. The data are from Fig. 6 and correspond to the intensities of the peaks. Excitation wavelengths are 295 nm (a), 300 nm (b), and 305 nm (c).

tallization, however, this does not mean that crystallization cannot be obtained. For a review of x-ray studies of glycoproteins, see Ref. 39.

All N-linked sugars, such as those of orosomucoid, contain a pentasaccharide Man_3 Glc NAc_2 core (Man, mannose; GlcNAc, *N*-acetylglucosamine). The heterogeneity of N-linked glycans originates primarily from the presence, absence, type, or length of the sugar side chains attached. The freedom of rotation around the glycosidic bonds induces a high flexibility of the molecules. Also, glycans are often solvent exposed on the protein surface, and in most glycoprotein structures known to date, only the 1-4 sugar residues most proximal to the glycosylation site are immobilized [39]. In orosomucoid, the carbohydrate side chains (largely *N*-acetylglucosamine and *N*-acetylneuraminic acid) exhibit broad ^{1}H NMR spectra resonances at 2.04 and 2.08 ppm [44]. The broad peak corresponds to a spin–spin relaxation time T_2 of 450 ms [45,46]. In NMR, the physical system is perturbed from its equilibrium condition by introducing an external magnetic field, and then the perturbing influence is removed. The system will then return to its original equilibrium condition. However, it does not return instantaneously, but takes a finite time to readjust to the changed conditions. The system is said to relax with a relaxation time T. If T is small, relaxation is fast, whereas if T is large, relaxation is slow. The internal fluctuating magnetic field which causes relaxation owes its existence to Brownian motion, characterized by the rotational correlation time τ_c. In solution, the relaxation time is long when τ_c is short and becomes shorter as τ_c increases [47]. For a relaxation time of 450 ms, the τ_c value is near 0.1 ns. The rotational correlation time of orosomucoid is equal to 17 ns [19]. Thus, the carbohydrate side-chain residues are highly mobile compared to the protein.

In crystals of glycoproteins, the electron density of the glycans can be obtained, when their mobility is decreased. This decrease was observed when glycans bridge two identical proteins [27–29] or two subunits of a protein such as the IgG F_c dimer [25,26].

In crystals of orosomucoid–progesterone complex, the proteins are linked together with the glycans (J. R. Albani and R. Martinez, paper in preparation). This protein–protein interaction is strong, inducing a decrease in the global rotation of the whole system and thus allowing observation of the electron density of the system.

The fluorescence excitation and emission spectra of the crystals (Figs. 2 and 3a, respectively) are characteristic of the fluorescence of Trp residues in proteins. The position of the emission peak (331 nm) and the value of the bandwidth (43 ± 1 nm) are typical for proteins containing tryptophan residues in a hydrophobic environment [33]. In fact, the characteristics of the emission spectrum of the crystals of orosomucoid–progesterone complex are identical to those observed in solution for the two buried Trp residues in the orosomucoid–progesterone complex. Therefore, the two Trp residues buried in the protein core have the same microenvironment in crystal and in solution.

Since the fluorescence emission spectrum of the crystals is characteristic of Trp residues buried in the

protein core, this means that the fluorescence of the surface Trp residue is completely quenched. This result may be explained by the fact that the protein–protein interaction in the crystal occurs via the surface of the protein. The Trp residue at the surface will be in contact with two proteins, facilitating high energy transfer to the neighboring amino acids. This result is in good agreement with that found by x-ray diffraction studies, i.e., the proteins are linked together at their surface by the glycans (J. R. Albani and R. Martinez, paper in preparation).

The red-edge excitation spectra method is very sensitive to the changes that occur in the microenvironment of the Trp residues. For example, Trp residues of intact lens protein from rat exhibit an emission shift of 14 nm upon varying the excitation from 290 to 308 nm. Photodamaging the lens induces an emission shift of 24 nm [48]. We also found that by modifying the method of preparation of orosomucoid, we were able to obtain a protein that has the same secondary structure as the one described in the present work, but with an altered Trp residue microenvironment exhibiting restriction of motions. The emission maximum of the fluorophore shifts from 337 to 347 nm upon excitation from 295 to 305 nm [21].

In crystals of orosomucoid–progesterone complex, the absence of a shift in the emission indicates that the microenvironment of the buried Trp residues exhibits residual motions (Fig. 5). This result is identical to that observed in solution for orosomucoid–progesterone complex), since we found a residual motion for the two buried Trp residues [11]. However, in solution and in the presence of progesterone, the resistance to rotation of the buried Trp residues is less important than that of the surface Trp residue [10,11]. Thus, an emission from two different relaxed states cannot be excluded, i.e., the emission of the buried Trp residues will occur from a relaxed state of lower energy than that of the emission of the surface Trp residue. Then an equilibrium occurs quickly so that it is difficult to separate the emission of each relaxed state. Therefore, upon red-edge excitation, no shift in the emission is observed.

In the crystals, we are observing the emission from the two buried Trp residues, only. Therefore, the red-edge excitation spectra method deals with the dynamics of the protein core. Since no red-edge excitation shift is observed in the crystal emission, the dipolar relaxation of the microenvironment of the two buried Trp residues, is fast. This could be explained by the water content of the protein crystal (35%). Therefore, crystallization of orosomucoid does not modify the structure and the dynamics of the protein core. However, we do not know from our experiments whether or not the two Trp residues have the same degree of freedom. Also, one may not exclude that, in solution and in crystal, the fluorescence of one of the two buried Trp residues could be completely quenched.

The fact that the emission maximum does not change upon rotation of the crystal (Fig. 6) is, in our case, another proof that the emission occurs from the buried Trp residues. Otherwise, we would observe a shift to 345 nm and an increase in the bandwidth, if at certain angles we are observing an emission from the Trp residue of the surface. The fluorescence intensity dependence on the angles of rotation of the crystals (Fig. 7) is the result of the motion of at least one Trp residue. This motion will modify the orientation of the corresponding dipole and thus will affect its absorption and its emission. More accurate change in the fluorescence intensity would be obtained if the angular variation is 5 instead of 45°. Unfortunately, we do not at present have the equipment for such an experiment.

Fluorescence intensities of the Trp residues in orosomucoid decay as a sum of three exponentials with lifetimes equal to 0.35 ± 0.03, 1.66 ± 0.07, and 4.64 ± 0.34 ns, and the corresponding amplitude fractions are 0.39 ± 0.05, 0.54 ± 0.03, and 0.07 ± 0.01, respectively ($\lambda_{em} = 330$ nm). $\bar{\tau}_0 = 2.23$ ns [49]. Recently, we attributed the two long lifetimes (1.42 and 3.61 ns) measured for the asialylated orosomucoid to the Trp residues embedded in the protein core and to the Trp residue of the surface, respectively [10,11].

The multiexponential decay may have different origins such as the emission from different relaxed states or the emission from different rotamer conformations. Also, the dynamics of the Trp residues within their microenvironments or the presence of two protein isoforms can induce different fluorescence lifetimes.

It has been shown that orosomucoid exhibits genetic polymorphism and that amino acid sequences may vary within a single individual. Thus, one should not exclude the possibility of having three lifetimes originating from Trp residues that emit from three orosomucoid isoforms. However, multiexponential decay is frequently observed for numbers of proteins that do not exhibit genetic polymorphism. Also, since all the orosomucoid preparations always give three lifetimes that are identical from one preparation to another, the possibility of an emission from two or three orosomucoid isoforms is to be excluded. This possibility was also excluded by studying the interaction between orosomucoid and TNS [49].

The rotamer model proposes that the Trp side chain may adopt low-energy conformations, due to rotation around the C_α–C_β and/or the C_β–C_γ bonds of the side chains [50], with each conformation displaying a distinct

decay time. In this model, if, for example, a protein contains one Trp residue that exhibits three fluorescence lifetimes such as is the case for the Trp residue in Erabutoxin b (3EBX), we should have at least three Trp side–chain rotamer conformations (contained in separate protein molecules [51]). But what about the dynamics of this Trp residue? The authors clearly indicate that the time-resolved data for 3EBX in solution at 300—nm excitation were consistent with those measured at 295 nm. In other words, upon increasing the excitation wavelength, no shift in the emission maximum or in the center of gravity of the spectrum of the Trp residue was observed. Thus, the authors clearly show in their work that the Trp residue in 3EBX displays residual motions. Therefore, since the fluorescence emission of the Trp residue in the crystal is similar to that observed in solution upon excitation at 295 nm, one should expect to obtain identical data in the crystal and in solution when excitation is performed at 300 nm. The absence of a red shift in the emission of Trp residues upon variation of the excitation wavelength clearly means that the microenvironment of the fluorophore is mobile. This mobility could induce that of the fluorophore itself. The dynamics of the Trp residue on the nanosecond time scale will modify the orientation and the intensity of the fluorophore dipole with time. The absorption and thus the emission of the fluorophore will vary with the dipole orientation. This local dynamics would affect the lifetime measurements.

The rotamer model does not take into consideration the interaction of the Trp residues with the surrounding microenvironments or the dynamics of the Trp residues and of their microenvironments. This model is not sufficient by itself to explain the origin of the fluorescence lifetimes or any other fluorescence observables. One also should not forget that the structure and the dynamics of the Trp microenvironment differ from one protein to another. And if the fluorescence observables including the fluorescence lifetime are independent of the structure and the dynamics of the microenvironment of the Trp residue, one should always measure the same values. Only denaturation of proteins results in uniform lifetimes near 2.5 ns, indicating that the structure and the dynamics of the tertiary structure, and not the amino acid sequence, are the origin of the varied fluorescence lifetimes among native proteins [52]. Therefore, if the origin of fluorescence lifetimes of Trp residues in proteins has to be explained by the rotamer model, one should complete the definition of this model by saying that energy conformations adopted by the Trp side chain are dependent on the structure and the dynamics of the surrounding microenvironment.

Emission from different relaxed states arises from the dynamics of the microenvironment of the fluorophore. We recently found that the dynamics and the structure of the microenvironment of the Trp residues and the tertiary structure of the protein have an important effect on the fluorescence intensity, the position of the maximum of the center of gravity, and the dependence of the anisotropy on the emission and excitation wavelengths [21].

Conclusion

The aim of this work was to show that it is possible to crystallize a glycoprotein containing 40% carbohydrate, such as orosomucoid, and to study its structure and dynamics. Our red-edge excitation spectra studies indicate that the structure and the dynamics of the core of the protein in the cystal are identical to those obtained in solution. Thus crystallization of orosomucoid does not affect the structure and the dynamics of the protein core. The fact that the fluorescence spectrum of orosomucoid–progesterone complex in the crystal has the same characteristic as that observed for the two buried Trp residues when the protein–ligand complex is in aqueous solution indicates that, in the crystal, the fluorescence of the surface Trp residue is quenched, as the result of the tight linkage between two neighboring molecules of orosomucoid (J. R. Albani and R. Martinez, paper in preparation). Interaction between the Trp residue at the protein surface and the neighboring amino acid residues increases energy transfer from the Trp residues to the other amino acid residues.

Our next goal is to measure the fluorescence lifetime of the Trp residues and to obtain the decay-associated spectra. This will allow us to compare the results obtained on the crystal to those obtained in solution, in the hope that more information can be obtained on the structure and the dynamics of orosomucoid.

ACKNOWLEDGMENTS

The author wishes to thank the referees for their constructive criticisms.

REFERENCES

1. T. Kute and U. Westphal (1976) *Biochim. Biophys. Acta* **420**, 195–213.
2. K. Schmid, H. Kaufmann, S. Isemura, F. Bauer, J. Emura, T. Motoyama, M. Ishiguro, and S. Nanno (1973) *Biochemistry* **12**, 2711–2724.

3. M. L. Friedman, K. T. Schlueter, T. L. Kirley, and H. B. Halsall (1985) *Biochem. J.* **232**, 863–867.
4. I. Nicollet, J.-P. Lebreton, M. Fontaine, and M. Hiron (1981) *Biochim. Biophys. Acta* **668**, 235–245.
5. Z. Wroblewski and W. Mijbaum-Katzenellenbogen (1984) *Acta Biochim. Polon.* **31**, 17–24.
6. G. Sager, O. G. Nilsen, and S. Jackobsen (1979) *Biochem. Pharmacol.* **28**, 905–911.
7. M. Canguly, R. H. Carnigham, and U. Westphal (1967) *Biochemistry* **6**, 2803–2814.
8. M. Kodicek, A. Infanzon, and V. Karpenko (1995) *Biochim. Biophys. Acta* **1246**, 10–16.
9. G. Weber, S. F. Scarlata, and M. Rholam (1984) *Biochemistry* **23**, 6785–6788.
10. J. R. Albani (1996) *Biochim. Biophys. Acta* **1291**, 215–220.
11. J. R. Albani (1997) *Biochim. Biophys. Acta* **1336**, 349–359.
12. J. R. Lakowicz and H. Cherek (1981) *Biochem. Biophys. Res. Commun.* **99**, 1173–1178.
13. R. F. Chen (1967) *Anal. Biochem.* **19**, 374–387.
14. J. R. Lakowicz and S. Keating-Nakamoto (1984) *Biochemistry* **23**, 3013–3021.
15. Z. Wasylewski, H. Koloczek, A. Wasniowska, and K. Slizowska (1992) *Eur. J. Biochem.* **206**, 235–242.
16. S. Guha, S. S. Rawat, A. Chattopadhyay, and B. Bhattacharyya (1996) *Biochemistry* **35**, 13426–13433.
17. A. Sommer, F. Paltauf, and A. Hermetter (1990) *Biochemistry* **29**, 11134–11140.
18. A. S. Ladokhin, L. Wang, A. W. Steggles, and P. W. Holloway (1991) *Biochemistry* **30**, 10200–10206.
19. J. R. Albani (1994) *J. Biochem.* **116**, 625–630.
20. J. R. Albani (1996) *J. Fluoresce.* **6**, 199–208.
21. J. R. Albani (1998) *Spectrochim. Acta* Part A, 175–183.
22. K. Schmid (1953) *J. Am. Chem. Soc.* **75**, 60–68.
23. A. P. Demchenko (1994) *Biophys. Biochim. Acta* **1209**, 149–164.
24. J. Deisenhofer (1981) *Biochemistry* **20**, 2361–2370.
25. B. J. Sutton and D. C. Phillips (1983) *Biochem. Soc. Trans.* **11**, 130–132.
26. T. H. Tahirov, T.-H. Lu, Y.-C. Liaw, Y.-L. Chen, and J.-Y. Lin (1995) *J. Mol. Biol.* **250**, 354–367.
27. B. Shaanan, H. Lis, and N. Sharon (1991) *Science* **254**, 862–866.
28. J. N. Varghese and P. M. Colman (1991) *J. Mol. Biol.* **221**, 473–486.
29. B. W. Matthews (1968) *J. Mol. Biol.* **33**, 491–497.
30. K. Miki, T. Ezoe, A. Masui, T. Yoshisaka, M. Mimuro, T. Fujiwara-Arasaki, and N. Kasai (1990) *J. Biochem.* **108**, 646–649.
31. A. Kita, N. Kasai, S. Kasai, T. Nakaya, and K. Miki (1991) *J. Biochem.* **110**, 748–750.
32. S. Harada, K. Kitadokoro, T. Kinoshito, Y. Kai, and N. Kasai (1991) *J. Biochem.* **110**, 46–49.
33. E. A. Burstein, N. S. Vedenkina, and M. N. Ivkova (1973) *Photochem. Photobiol.* **18**, 263–275.
34. J. Albani (1992) *Biophys. Chem.* **44**, 129–137.
35. G. Weber (1960) *Biochem. J.* **75**, 335–345.
36. P. S. Song and W. E. Kurtin (1969) *J. Am. Chem. Soc.* **91**, 4892–4906.
37. Y. Yamamoto and J. Tanaka (1972) *Bull. Chem. Soc. Jpn.* **45**, 1362–1366.
38. M. R. Eftink (1991) *Methods Biochem. Anal.* **35**, 127–205.
39. D. F. Wyss and G. Wagner (1996) *Curr. Opin. Biotechnol.* **7**, 409–416.
40. F. Labeyrie and A. Baudras (1972) *Eur. J. Biochem.* **25**, 33–40.
41. M. Gervais, Y. Risler, and S. Corazzin (1983) *Eur. J. Biochem.* **130**, 253–259.
42. Z.-X. Xia and F. S. Mathews (1990) *J. Mol. Biol.* **212**, 837–863.
43. J. R. Albani (1997) *Photochem. Photobiol.* **66**, 72–75.
44. J. D. Bell, J. C. Brown, J. K. Nicholson, and P. J. Sadler (1987) *FEBS Lett.* **215**, 311–315.
45. B. Fournet, J. Montreuil, G. Strecker, L. Dorland, J. Haverkamp, J. F. G. Vliegenthart, J. P. Binette, and K. Schmid (1978) *Biochemistry* **17**, 5206–5214.
46. K. Akiyama, E. R. Simons, P. Bernasconi, K. Schmid, H. Van Halleck, J. F. G. Vliengenthart, H. Haupt, and G. H. Schwick (1984) *J. Biol. Chem.* **259**, 7151–7154.
47. J. W. Akitt (1983) in *NMR and Chemistry. An Introduction to the Fourier Transform Multinuclear Era*, Chapman and Hall, Ltd., New York, pp. 61–69.
48. Ch. Mohan Rao, S. Chenchal Rao, and P. Bheema Rao (1989) *Photochem. Photobiol.* **50**, 399–402.
49. J. Albani, R. Vos, K. Willaert, and Y. Engelborghs (1995) *Photochem. Photobiol.* **62**, 30–34.
50. H. L. Gordon, H. C. Jarrell, A. G. Szabo, K. J. Willis, and R. L. Somorjai (1992) *J. Phys. Chem.* **96**, 1915–1921.
51. T. E. S. Dahms, K. J. Willis, and A. G. Szabo (1995) *J. Am. Chem. Soc.* **117**, 2321–2326.
52. A. Grinvald and I. Z. Steinberg (1976) *Biochim. Biophys. Acta* **427**, 663–678.